

1 Seasonal Dynamics of *Anopheles stephensi* and its 2 Implications for Mosquito Detection and Emergent Malaria 3 Control in the Horn of Africa

4 Charles Whittaker^{1,‡}, Arran Hamlet¹, Ellie Sherrard-Smith¹, Peter Winskill¹, Gina Cuomo-
5 Dannenburg¹, Patrick G.T. Walker¹, Marianne Sinka², Samuel Pironon^{3,4}, Ashwani Kumar⁵, Azra
6 Ghani¹, Samir Bhatt^{1,6†}, Thomas S. Churcher^{1†}

7 ¹MRC Centre for Global Infectious Disease Analysis & Abdul Latif Jameel Institute for Disease and Emergency Analytics,
8 School of Public Health, Imperial College London, London, UK

9 ²Department of Biology, University of Oxford, Oxford, UK

10 ³Royal Botanic Gardens Kew, Richmond, Surrey, UK

11 ⁴United Nations Environment Program World Conservation Monitoring Centre, Cambridge, UK

12 ⁵Vector Control Research Centre, Indira Nagar, Puducherry, India

13 ⁶Section of Epidemiology, Department of Public Health, University of Copenhagen, Copenhagen, Denmark

14 [†]These authors jointly supervised this work.

15 ***Corresponding Author:** Charles Whittaker, Department of Infectious Disease Epidemiology, School of Public Health, Imperial
16 College, London W2 1PG, United Kingdom. Email: charles.whittaker16@imperial.ac.uk

17 **Keywords:** *Anopheles stephensi*; malaria ecology; urban malaria; population dynamics;
18 seasonality; epidemiology.

19 Abstract

20 Invasion of the malaria vector *Anopheles stephensi* across the Horn of Africa threatens
21 control efforts across the continent, particularly in urban settings where the vector is able to
22 proliferate. Malaria transmission across Africa is primarily determined by the abundance of
23 dominant vectors, which often varies seasonally with rainfall. However, it remains unclear
24 how *An.stephensi* abundance changes throughout the year, despite this being a crucial input
25 to surveillance and control activities. We collate longitudinal catch-data from across its
26 endemic range to better understand the vector's seasonal dynamics and explore the
27 implications of this seasonality for malaria surveillance and control across the Horn of Africa.
28 Our analyses reveal pronounced variation in seasonal dynamics, the timing and nature of
29 which are poorly predicted by rainfall patterns. Instead, they are associated with temperature
30 and patterns of land-use, with seasonality frequently differing between rural and urban
31 settings. Our results show that timing entomological surveys to coincide with rainy periods is
32 unlikely to improve the likelihood of detecting *An.stephensi*. Integrating these results into a
33 model of malaria transmission, we show that timing indoor residual spraying campaigns to
34 coincide with peak rainfall offers little improvement in reducing disease burden compared to
35 starting in a random month. Our results suggest that unlike other major malaria vectors in
36 Africa, rainfall may be a poor guide to predicting the timing of peaks in *An.stephensi*-driven
37 malaria transmission. This highlights the urgent need for longitudinal entomological
38 monitoring of the vector in its new environments given recent invasion and potential spread
39 across the continent.

40

41 Introduction

42 There has been an estimated 40% reduction in the burden of malaria since 2000,
43 predominantly due to significant scale-up of control interventions¹. Increasing urbanisation of
44 Africa's human population (31% to 43% between 1990 and 2018, with >60% expected to live
45 in urban areas by 2050²) is also thought to have indirectly contributed to reductions in
46 disease burden. Previous work has found significantly lower Entomological Inoculation Rates
47 (EIR) in urban compared to rural settings^{3,4}. This is thought to be underpinned by factors
48 including differences in housing quality^{5,6}, reduced suitability of habitats for *Anopheles*
49 breeding in urban settings⁷⁻⁹, better access to treatment¹⁰, and higher population densities
50 leading to lower mosquito-to-human ratios (and reduced transmission)¹¹. Whilst these trends
51 are not always consistently identified^{12,13} (including previous work showing some vectors can
52 adapt to urban environments¹⁴), increasing urbanicity across Africa is anticipated to
53 complement planned scale-up of malaria control interventions aimed at achieving the targets
54 outlined in the World Health Organization's 2030 Global Technical Strategy for Malaria¹⁵.

55 This beneficial impact of increasing urbanization on malaria burden is contingent on urban
56 settings remaining areas of comparatively low transmission. This is currently under threat in
57 Africa because of the invasion and establishment of *An. stephensi*, a malaria vector that is
58 potentially capable of thriving in urban areas of the continent¹⁶. There are three known forms
59 of the species ("type", "intermediate" and "mysorensis") found across its native range in
60 South Asia. The mysorensis form is predominantly found in rural settings, is highly zoophilic
61 and typically possesses a low vectorial capacity¹⁷. By contrast, the type and intermediate
62 forms represent efficient vectors capable of transmitting both *Plasmodium falciparum* and
63 *Plasmodium vivax*¹⁸⁻²⁰ in urban environments. This ability to proliferate in urban locations
64 distinguishes this species from other malaria vectors in sub-Saharan Africa, and is thought to
65 be underpinned by an increased tolerance for breeding in polluted water sources²¹, and
66 superior ability to utilise the purpose-built water storage tanks present in many urban
67 settings^{22,23}.

68 The African invasion by *An. stephensi* was first reported from Djibouti City in 2012²⁴ and has
69 since been recorded in Ethiopia^{18,25}, Sudan^{26,27}, Somalia²⁸ and Somaliland²⁹, with recent
70 work highlighting suitability of the continent's largest population centres (where >100 million
71 individuals live) as a habitat for this species¹⁶. Whilst causality has yet to be established,
72 emergence of *An. stephensi* is thought to have contributed to resurgence of malaria
73 transmission in Djibouti (10-fold increase in cases 2013-2019), highlighting the potential
74 threat that this vector poses to malaria control across the Horn of Africa³⁰ and the continent
75 more generally³¹.

76 Despite the significant public-health this vector poses, substantial uncertainty remains in how
77 its establishment might influence malaria dynamics in the region, particularly in the
78 (predominantly urban) settings where the disease is currently largely absent. A key driver of
79 this will be the vector's seasonal dynamics. Mosquito populations may show marked
80 variation in seasonal abundance, often exhibiting substantial annual fluctuations in size that
81 drive the temporal profile of disease risk. The efficacy of many malaria control interventions
82 (such as seasonal malaria chemoprevention³² (SMC), indoor-residual spraying³³ (IRS) or
83 larval source management³⁴ (LSM)) depends on optimally timing their delivery relative to
84 seasonal peaks in vector abundance. A better understanding of the seasonality of *An.*
85 *stephensi* across its current range will help guide entomological monitoring and surveillance

86 activities in areas of possible invasion and have material consequences for the effective
87 control of *An. stephensi* driven malaria transmission.

88 Here we systematically collate longitudinal catch data for *An. stephensi* across its endemic
89 range to better understand these dynamics. Our results highlight pronounced variation in the
90 extent and timing of seasonality (poorly predicted by patterns of rainfall), with distinct
91 dynamics separating rural and urban settings. We show that this variation has material
92 consequences for the effective design of entomological surveillance programmes.
93 Integrating these results with a previously published model of malaria transmission also
94 highlights how this variation will influence the efficacy of malaria control efforts in parts of the
95 Horn of Africa where the disease is currently (or has previously been) largely absent and
96 underscores the need for rapid scaleup of entomological monitoring across the region.

97 **Methods**

98 **Systematic Review of *Anopheles stephensi* Surveys**

99 We collated references from published systematic reviews of literature relating to
100 *An. stephensi*^{16,35}, and updated these previous searches by searching *Web of Science* and
101 *PubMed* from Jan.2017 to Sep.2020. We included all records containing temporally
102 disaggregated adult mosquito catch data with monthly (or finer) temporal resolution spanning
103 at least 10 months, that had not been conducted as part of vector control intervention trials
104 and where at least 25 *An. stephensi* mosquitoes had been caught over the study period. A
105 total of 36 references were collated containing 65 time-series with monthly catch data (no
106 study presented data at a finer temporal resolution) from surveys carried out across
107 Afghanistan, Djibouti, India, Iran, Myanmar and Pakistan. See **Supplementary Information**
108 for further details and references therein.

109 **Clustering of Similar Time-Series & Random Forest Prediction of Cluster Membership**

110 Following methodologies developed in previous work³⁵, we fitted a Gaussian Process-based
111 model to smooth these mosquito count time-series, using a Negative Binomial likelihood to
112 account for overdispersion and a periodic kernel function to capture the repeating patterns
113 often observed seasonally in mosquito populations. Model fitting was carried out within a
114 Bayesian framework, using the probabilistic programming language STAN³⁶. We then
115 calculated summary statistics for each smoothed time-series to characterise their temporal
116 properties (**Supplementary Information**), generating a set of parameters for each time-
117 series that summarises their temporal properties. We then scaled and normalised each
118 summary statistic to give a mean 0 and unit variance – a process necessary for the principal
119 components analysis (PCA) we apply to identify a lower-dimensional representation of the
120 structure present in the data amenable to visualisation.

121 Using *k*-means clustering, we identified clusters of time-series with similar temporal
122 properties – the output of this process is a label for each time-series indicating which cluster
123 (of time-series with similar temporal properties) each specific time-series was assigned to.
124 For each study location, we extracted a suite of satellite-derived environmental variables
125 (**Supplementary Table 2**) and used these variables alongside empirically calculated rainfall
126 seasonality and average monthly catch as covariates within a random-forest based
127 classification framework to predict cluster membership of each time-series. These models
128 were fitted using the R package *Ranger*³⁷ with 6-fold cross-validation utilised to optimise
129 hyperparameters. Results are based on averaging the results of 25 iterations of cross-

130 validation and model fitting and predictions made using out-of-bag estimates. There were
131 significant imbalances in class size across clusters and so we carried out upsampling using
132 the SMOTE³⁸ algorithm. For results without upsampling see **Supplementary Information**.

133 **Probability of Detecting *Anopheles stephensi* With Different Surveillance Strategies**

134 We explore the implications of seasonal variation in *An. stephensi* abundance on the
135 probability of detecting the vector in entomological surveys using a theoretical sampling
136 method with a defined amount of effort (such as a human landing catch conducted by a
137 single volunteer for one night). We use a statistical framework (described further in
138 **Supplementary Information**) that calculates the cumulative probability of detection from: i)
139 an overall assumed *An. stephensi* annual biting rate (ABR, arbitrarily set to 20 for illustrative
140 purposes here); ii) changes in vector density over the course of the year (from our collated
141 time-series); and iii) various factors relating to timing of, and effort expended in, the
142 entomological survey. Specifically, for each time-series, we identified the month with the
143 highest rainfall, and the month in which vector density was highest (noting that these months
144 were very rarely the same month). We then calculated the cumulative probability of *An.*
145 *stephensi* detection using the framework, under a range of different surveillance strategies.
146 Specifically, three strategies were simulated:

- 147 • **Vector-Peak Timed:** Starting the survey at the month with peak vector density
148 (noting that in the absence of pre-existing detailed entomological information this is a
149 hypothetical quantity designed to illustrate an approximate upper bound on the
150 detection probability that could be achieved).
- 151 • **Rainfall-Peak Timed:** Starting the survey at the month with peak rainfall.
- 152 • **Random Month Timed:** The expected probability of detection achieved if the survey
153 was started during a random month (calculated by simulating survey starting in each
154 of the year's 12 months and calculating the average cumulative probability).

155 In addition to varying the survey's starting time, we also varied the amount of sampling effort
156 (number of days sampled within each month) and overall duration of the survey (consecutive
157 months sampled given a defined number of nights sampling per month). Note that the aim
158 here is not to describe the exact probability of missing *An. stephensi* in any given
159 entomological survey, as this will depend on a wide array of other, poorly defined and
160 heterogeneous factors (e.g. type of catch methodology used, location etc). We also assume
161 that the collection method is unbiased (i.e. not biased towards catching mosquitoes with
162 particular resting or biting properties) which is also highly unlikely. Instead, the aim is to
163 highlight how variation in seasonal dynamics can influence the nature of surveillance
164 required to successfully detect a single *An. stephensi* (i.e. successfully establish presence),
165 and the probability of detection should be viewed as a relative measure (i.e. viewed in
166 relation to other sampling efforts and survey timings possible for surveys) and not an
167 absolute value. Note that this framework assumes no seasonal variation in factors other than
168 mosquito abundance (such as the ability of the sampling method to accurately record ABR)
169 that might influence the probability of *An. stephensi* being caught by our theoretical sampling
170 method.

171 **Modelling *Anopheles stephensi*-Driven Malaria Dynamics and Control**

172 We integrated these vector abundance time-series into a published population-level model of
173 *Plasmodium falciparum* malaria transmission and disease dynamics³⁹⁻⁴¹ to explore the
174 implications of *An. stephensi* seasonality on malaria control in settings in the Horn of Africa

175 where malaria is currently largely absent (see **Supplementary Information** for full
176 description of the modelling framework). We use the modelling framework to understand
177 how variation in mosquito seasonality might influence the impact of IRS, a key vector control
178 intervention. As the dynamics of *An. stephensi*'s establishment and influence on temporal
179 trends in malaria transmission during its establishment remain unclear, we focused on the
180 time-period immediately following establishment (when the disease is at equilibrium) and
181 provide an illustrative example of how seasonality of *An. stephensi* driven malaria
182 transmission could influence the effectiveness of IRS in a site with no pre-existing history of
183 malaria control. For simplicity we assume that all transmission is due to *An. stephensi* and
184 that IRS efficacy against this species is consistent with that observed against other species
185 across the continent⁴². We simulate the impact of a single, illustrative IRS spraying
186 campaign in a setting with an annual EIR of 1.5 (average malaria prevalence of 8-9%), timed
187 either for optimal impact, randomly or alongside peak rainfall, and assume that 80% of the
188 vector's resting sites are successfully sprayed (noting the vector is thought to also rest in
189 animal houses which are not typically sprayed in public-health campaigns). For further
190 details, see **Supplementary Information**.

191 **Results**

192 **Diversity in Temporal Dynamics Across the Collated *Anopheles stephensi* Time-**
193 **Series:** A total of 65 time-series from across Afghanistan, Djibouti, India, Iran, Myanmar and
194 Pakistan were identified (**Fig.1A, Supp Fig.1**). Substantial variation in the degree and timing
195 of vector seasonality was observed, with the maximum percentage of annual vector density
196 in any consecutive 4-month period (a proxy for degree of seasonality) ranging from 35-99%
197 across the collated studies (average=62%). This contrasted with rainfall seasonality, where
198 highly seasonal rainfall patterns were consistently observed across the locations the surveys
199 had been carried out in (maximum percentage of annual rainfall in any consecutive 4-month
200 period, mean=82, range 47-99%). We also observed a diverse range of temporal patterns,
201 ranging from highly seasonal dynamics with a single seasonal peak, to bimodal population
202 dynamics with two peaks within a single year, or more perennial patterns of abundance
203 (**Fig.1B**).

204 **Statistical Characterisation and Clustering of Temporal Properties Highlights Distinct**
205 **Archetypes:** Summary statistics were calculated for each time-series to characterise their
206 temporal properties (**Supp Fig.2**), followed by k-means clustering of the results to cluster the
207 time-series into groups with similar temporal patterns. Our results highlight two distinct
208 clusters of time-series, each characterised by distinct temporal patterns (**Fig.2B**). Cluster 1
209 time-series had single seasonal peaks and were more seasonal (average of 68% of annual
210 vector density in the consecutive 4-month period with highest density) than Cluster 2 time-
211 series, which had more perennial patterns of annual abundance (average 44% of annual
212 vector density in the consecutive 4-month period with highest density) and contained several
213 time-series with two peaks across the year. Despite differing significantly in mean vector
214 abundance seasonality (**Fig.2C and 2D**, $p<0.001$), there was no significant difference
215 between Clusters in rainfall seasonality (**Fig.2D**, $p=0.59$). Seasonality of rainfall (defined as
216 the highest proportion of total annual rainfall occurring in any consecutive 4 month period)
217 across sampled locations was high (average 82% and 84% for Clusters 1 and 2
218 respectively) despite wide variation in vector abundance seasonality. Timing of peak rainfall
219 relative to peak vector density significantly differed between clusters (**Supp Fig.3**), with peak
220 rainfall and vector abundance separated by <1 month on average for Cluster 1 compared to

221 2.2 months for Cluster 2. There was, however, considerable within-cluster variation in
222 timing—within Cluster 1, timing of peak vector density relative to rainfall ranged from -5.8
223 months to +5.3 months (with 6 months the maximum gap that can occur within an annually
224 repeating 12 month time-series, highlighting that the peaks in vector density relative to
225 rainfall were found across the entirety of the year). We also explored varying the number of
226 clusters specified in the k-means algorithm. Specifying 4 clusters resulted in further
227 disaggregation of the 49 time-series in Cluster 1 into 3 separate clusters, each characterised
228 by a single seasonal peak, but which differed in the timing of peak vector-density relative to
229 peak rainfall (**Supp Fig.4**).

230 **Random-Forest Modelling of Seasonal Dynamics Highlights Urbanicity as a Key**
231 **Factor:** We fitted a random forest-based classification framework to predict cluster
232 membership (Cluster 1 or Cluster 2, as defined in **Fig.2A**). Due to the significant class size
233 imbalance between Cluster 1 (n=49) and Cluster 2 (n=16), we up-sampled Cluster 2 data to
234 generate balanced classes. Across 25 iterations of random forest model fitting, mean AUC
235 was 0.89 (indicating good predictive performance) and the model was able to correctly
236 classify Cluster 1 and Cluster 2 time-series equally well (83% and 85% accuracy
237 respectively).

238 We calculated the relative importance of each variable to the model's predictive ability
239 (**Fig.2E**). Patterns of land-use were strongly associated with different clusters—time-series
240 from surveys in locations with lower population density (a proxy for rurality) more likely to
241 belong to Cluster 2 (less seasonal), as were areas with a high proportion of land occupied by
242 irrigated cropland. By contrast, a high proportion of land occupied by rainfed cropland was
243 associated with Cluster 1 (more seasonal) dynamics. We also observed strong associations
244 with temperature covariates, including the mean temperature of the driest quarter (where a
245 high temperature was associated with Cluster 2), temperature seasonality (where a non-
246 monotonically increasing relationship was observed, see **Fig.2E inset panels** and **Supp**
247 **Fig.5** for all covariate response plots) and whether the study had been conducted in Iran
248 (indicating potential spatial confounding). By contrast, rainfall seasonality was not an
249 important predictor of temporal dynamics and was in the least 5 important variables.
250 Examining the association between cluster membership and rurality/urbanicity (defined by
251 study authors), there was indication of an association (chi-squared test, $p=0.07$), though this
252 was not statistically significant at the 5% level. 88% (n=22/25) time-series from urban
253 settings were assigned to Cluster 1, and only 12% (n=3/25) assigned to Cluster 2. 65%
254 (n=24/37) of time-series from rural settings were assigned to Cluster 1, and 35% (n=13/37)
255 to Cluster 2.

256 Model predictive performance and variable importance rankings were similar when no up-
257 sampling was applied (AUC=0.81, **Supp Fig.6**), though predictive accuracy was highly
258 unbalanced (Cluster 2 accuracy=50%, Cluster 1 accuracy=94%). Model performance and
259 variable importance ordering remained similar when fitting the model and explicitly holding
260 out a subset of the data to subsequently evaluate model performance (n=7 time-series,
261 **Supp Fig.7**). Predictive power for seasonality (percentage of vector catch in any 4-month
262 period) was more modest, although estimates were positively correlated ($r=0.43$, **Supp**
263 **Fig.8**).

264 **Implications of Seasonal Dynamics for Entomological Surveillance of *Anopheles***
265 ***stephensi* across the Horn of Africa:** We collated the same covariates for countries across
266 the Horn of Africa and used the random forest model to predict cluster membership and

267 potential temporal dynamics of *An. stephensi* across the region (**Fig.3A**). Our results
268 highlight distinct geographical areas considered more likely to belong to Cluster 1 (more
269 seasonal) and Cluster 2 (less seasonal), as well as areas of significant uncertainty. We next
270 asked what consequences this seasonality might have on entomological surveillance of the
271 vector, with a focus on how these seasonal dynamics might interact with features of
272 surveillance programmes such as the timing and duration of entomological surveys. Across
273 the collated temporal profiles, in a setting with an ABR of 20, surveys consisting of 3 months
274 sampling and 3 sampling days per month that were timed to start at periods of peak *An.*
275 *stephensi* density were on average 64% more likely to detect the vector compared to starting
276 the survey at a random month of the year; and 57% more likely to successfully detect the
277 vector compared to starting the survey in the month of peak rainfall (**Fig.3B**). Timing
278 entomological surveys to coincide with peaks in rainfall did not lead to a significant increase
279 in the probability of successfully detecting *An. stephensi* (average 4% increase), suggesting
280 that the timing of peak rainfall may be a poor measure for guiding entomological surveys
281 searching for the vector. We next stratified these results by temporal Cluster (**Fig.3C**). For
282 Cluster 1 (and a survey lasting 3 months, with 3 days sampling per month) we observed
283 differences in the cumulative probability of detection when comparing strategies which start
284 surveys at the location's rainfall peak, compared to starting them at peak *An. stephensi*
285 abundance – on average, the latter strategy increased the cumulative probability of detection
286 by 62% compared to a randomly timed survey, compared to only a 40% increase over
287 random timing for Cluster 2.

288 **Modelling the Impact of *Anopheles stephensi* Seasonality On Vector Control**
289 **Measures:** Integrating the temporal profiles of *An. stephensi* abundance with a malaria
290 transmission model, we explored how variation in temporal dynamics influences the impact
291 of IRS (with two different insecticides, **Fig.4A**). Across the *An. stephensi* temporal profiles,
292 optimal timing of IRS delivery resulted in an average of 47.6% reduction in annual malaria
293 incidence in the 12 months following spraying for pirimithos methyl, and 28.9% for
294 bendiocarb (**Fig.4B**). These results represent 1.12x and 1.41x increases over the average
295 impact achieved if the campaign is timed to a random month of the year. The extent to which
296 optimal timing provided greater impact than random timing was dependent on the degree of
297 seasonality and insecticide however—it increased with the degree of seasonality and was
298 consistently larger for bendiocarb than pirimithos methyl (due to the latter's longer duration
299 and retention of residual activity following spraying). Timing the IRS campaign to occur when
300 rainfall peaks did not significantly increase impact compared to timing the campaign to a
301 random month (with less than a 2% average increase in impact for both pirimithos methyl
302 (**Fig.4C**) and bendiocarb (**Fig.4D**)) and had significantly lower impact than optimally timed
303 campaigns (39% and 15% lower impact for pirimithos methyl and bendiocarb respectively).

304 Discussion

305 Invasion and establishment of *An. stephensi* across the Horn of Africa represents an urgent
306 threat to malaria control in the region. Understanding the temporal profile of vector
307 abundance of the species will inform effective deployment of surveillance, monitoring and
308 control interventions aimed at mitigating this potential impact, particularly in urban settings
309 where malaria has historically been largely absent or only minimally present. Collating data
310 from across the vector's endemic range, we identify broad diversity in the extent and nature
311 of *An. stephensi* seasonal dynamics. This variation is associated with a wide array of

312 ecological factors, including seasonal fluctuations in temperature and patterns of land use,
313 including a potential role of urbanicity in shaping dynamics.

314 Our analyses identified population per km² as the most important predictor of cluster
315 membership, with high population density being strongly associated with Cluster 1 dynamics
316 (more seasonal patterns of abundance). This potential disparity in temporal dynamics across
317 rural and urban settings will likely have implications for both how resources aimed at
318 surveillance control should be targeted to these different settings, and the public health
319 impact of different control interventions. Our results suggest that urban *An. stephensi*
320 populations are likely to display more seasonal dynamics, supporting the utility of temporally
321 targeted interventions like short-lived IRS or LSM in these settings. The same is not
322 necessarily true in rural settings, where shorter duration control interventions are likely to be
323 impactful but may be less consistent in their effectiveness (without local surveys being
324 conducted to establish the timing and extent of seasonality) due to the range of seasonal
325 profiles observed, which included more perennial patterns of abundance. Implementing
326 these measures and achieving sufficient intervention population coverage in urban settings
327 is likely to present logistical challenges, given the historical absence of large-scale vector
328 control campaigns from urban communities. If these barriers can be surmounted however,
329 our results suggest such measures are likely to be impactful, though remaining uncertainty
330 around the degree of endophily *An. stephensi* can display⁴³ might necessitate alternative
331 interventions to IRS that are not dependent on resting behaviour, such as LSM³⁴.

332 Our results also suggest a limited role for rainfall in shaping the diverse temporal dynamics
333 across the collated *An. stephensi* catch-data, contrary to results observed for other Africa
334 malaria vector species (e.g. *An. gambiae*^{44,45}). Specifically, that areas with highly seasonal
335 rainfall may not have highly seasonal patterns of *An. stephensi* abundance. Instead, our
336 analyses highlight an association between temperature and seasonal patterns of abundance
337 with both temperature seasonality and the average temperature during the driest quarter
338 being highly predictive of dynamics. This is consistent with previous work identifying
339 temperature as a key driver of mosquito population dynamics, due to its impact on an array
340 of mosquito life-history traits including biting rate, lifespan and fecundity (amongst several
341 others)^{46,47}. It should be stressed however that these covariates identified here are not
342 necessarily predictive of absolute *An. stephensi* abundance in a region, but rather the
343 seasonality in abundance. A much more detailed sampling strategy considering variability in
344 the accuracy and biases of sampling methods and other geospatial methods will be needed
345 to identify whether the vector has invaded a region.

346 The work also highlights the exceptionally limited amount of longitudinally collected
347 entomological data from across *An. stephensi*'s current geographical range (including the
348 Horn of Africa region) that currently exists. In highly seasonal settings there is a risk of
349 erroneously concluding *An. stephensi*'s absence, particularly as the time of low vector
350 catches may not coincide with times of low rainfall, as is frequently the case for other
351 mosquitoes endemic to Africa. Longitudinal surveys enabling better description of these
352 dynamics would therefore be useful in enabling subsequent refinement and timing of shorter
353 surveys aimed at detecting presence only (whilst also providing additional information on
354 temporal dynamics that can facilitate the effective targeting and timing of interventions such
355 as IRS or LSM). Indeed, our results suggest that rainfall may provide a poor guide to timing
356 of intervention campaigns in settings where *An. stephensi* is the dominant vector,

357 underscoring the crucial role detailed entomological data collection and establishment of
358 patterns empirically will play in optimising vector surveillance and disease control efforts.

359 There are several important limitations to the work presented here. Firstly, we assume that
360 the inferred ecological relationships linking environmental features to temporal dynamics will
361 translate from the vector's historical range to the Horn of Africa. Indeed, our results highlight
362 significant plasticity and variation in *An. stephensi's* seasonal abundance depending on the
363 setting, and therefore the extent to which our results will extrapolate to new settings remains
364 unclear—making collection and analysis of longitudinal catch-data collected from the Horn of
365 Africa an urgent research priority. Relatedly, due to the limited amount of data available and
366 the wide geographical range over which the collated studies were conducted, we cannot rule
367 out possible spatial confounding in shaping the inferred associations. Analysis of the
368 distribution of locations stratified by rural/urban status and cluster assignment did not reveal
369 obvious patterns of spatial confounding (**Supp Fig.9**), though the study being conducted
370 from Iran was a high-ranking variable in the random forest model and it is possible some
371 degree of spatial confounding is present. We were also unable to consider is the possibility
372 of variation in temporal dynamics between *An. stephensi* forms. Identification of the *An.*
373 *stephensi* form is challenging, requiring close visual examination⁴⁸ or molecular methods⁴⁹.
374 Availability of this data was limited, and we lack the ability to disaggregate time-series by the
375 specific form caught and hence preclude form as a confounder of some of the identified
376 relationships linking environmental factors and temporal dynamics. Another limitation relates
377 to our usage of mosquito abundance data, which is highly prone to biases driven by the
378 collection method used. Whilst the analyses here use normalised mosquito counts (rather
379 than raw abundance), trapping method bias might vary between season, which could affect
380 the reliability of the seasonal patterns inferred, as well as introduce additional variation into
381 catch data not captured here and which would influence the results describing the probability
382 of detecting *An. stephensi* under different sampling effort and survey timing contexts.

383 We do not include insecticide resistance into our model of malaria transmission. Insecticide
384 resistance is well-documented for *An. stephensi*^{50–52}, and recent populations assayed in
385 Ethiopia showed resistance to all four major insecticide classes^{53,54}, suggesting that IRS
386 might have a lower impact than suggested here. Relatedly, we do not consider uncertainty in
387 *An. stephensi* bionomic properties (e.g timing of biting or whether resting occurs
388 predominantly indoors or outdoors), which might vary by season and could further modulate
389 the impact of interventions such as IRS where killing is mediated primarily through indoor
390 resting following feeding. Variation in *An. stephensi's* bionomic properties has previously
391 been identified⁵⁵, including a propensity for crepuscular biting and resting outside of houses
392 compared to other *Anopheles* species dominant in sub-Saharan Africa^{16,19,43} that might
393 render IRS less effective and necessitate consideration of other strategies such as LSM.
394 Whilst the aim of this work is to illustrate how seasonality modulates (rather than precise
395 estimates of) intervention impact, these considerations underscore the urgent need for a
396 more detailed characterisation of *An. stephensi* across the Horn of Africa to quantify its
397 bionomic properties and insecticide resistance profile more precisely in these settings, and
398 identify the most effective control interventions to deploy.

399 Our work highlights significant variation in temporal dynamics across *An. stephensi*
400 populations; variation that is shaped by distinct ecological factors, can markedly differ
401 between urban and rural settings, and which has material consequences for the
402 effectiveness of vector control interventions. Our work also highlights the need to better

403 understand the vector's dynamics in settings where it has newly established, and how these
404 dynamics might differ to other *Anopheles* species also present and capable of malaria
405 transmission. Indeed, the trajectory of *An. stephensi's* establishment and subsequent
406 dynamics in the Horn of Africa remains deeply unclear and the scarcity of published
407 entomological studies from the region underscores the need for studies longitudinally
408 surveying locations where *An. stephensi* has recently arrived. This will be important to
409 understanding the patterns of seasonal variation the vector displays, and support optimising
410 the delivery of malaria control interventions aiming to mitigate the impact of this invasive
411 vector.

412 **Data and Code Availability**

413 All data collated as part of this study and the code required to reproduce these analyses can
414 be found at the following link: <https://github.com/cwhittaker1000/stephenseasonality>.

415 **Acknowledgements and Funding Sources**

416 CW is supported by Sir Henry Wellcome Postdoctoral Fellowship, Ref 224190/Z/21/Z. This
417 research was funded in whole, or in part, by the Wellcome Trust (Ref 224190/Z/21/Z). For
418 the purpose of Open Access, the author has applied a CC BY public copyright licence to any
419 Author Accepted Manuscript version arising from this submission. SB & AG both
420 acknowledge grant support from the Bill and Melinda Gates Foundation. TSC and AH both
421 acknowledge Wellcome Trust (National Institute for Health Research–Wellcome Partnership
422 for Global Health Research Collaborative Award, 'Controlling emergent *Anopheles stephensi*
423 in Ethiopia and Sudan (CEASE), Ref: 220870_Z_20_Z). The work is supported by the MRC
424 Centre for Global Infectious Disease Analysis (reference MR/R015600/1) which is jointly
425 funded by the UK Medical Research Council (MRC) and the UK Foreign, Commonwealth &
426 Development Office (FCDO), under the MRC/FCDO Concordat agreement, the EDCTP2
427 programme supported by the European Union and Community Jameel. GCD acknowledges
428 funding from the Royal Society.

429 **Author Contributions**

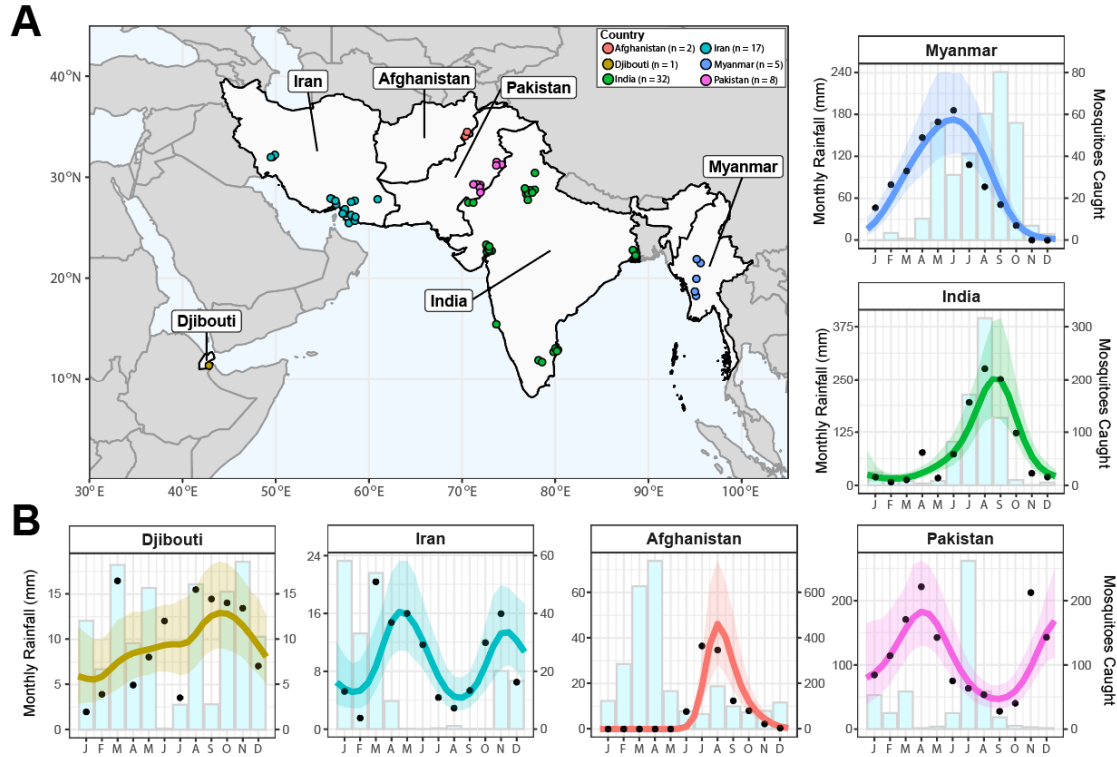
430 CW, AH and TC conceived the study. ESS and SB contributed to the design of the study.
431 CW carried out the systematic review. CW and SB developed the underlying statistical
432 framework, with input on the analyses from AH, AG, TC, GCD, PGTW, PW and ESS. CW
433 wrote the first draft manuscript, with all authors providing feedback and suggestions during
434 manuscript drafting. All authors approved the final version of the manuscript.

435

436

437

438



439

440

441

442

443

444

445

446

447

448

449

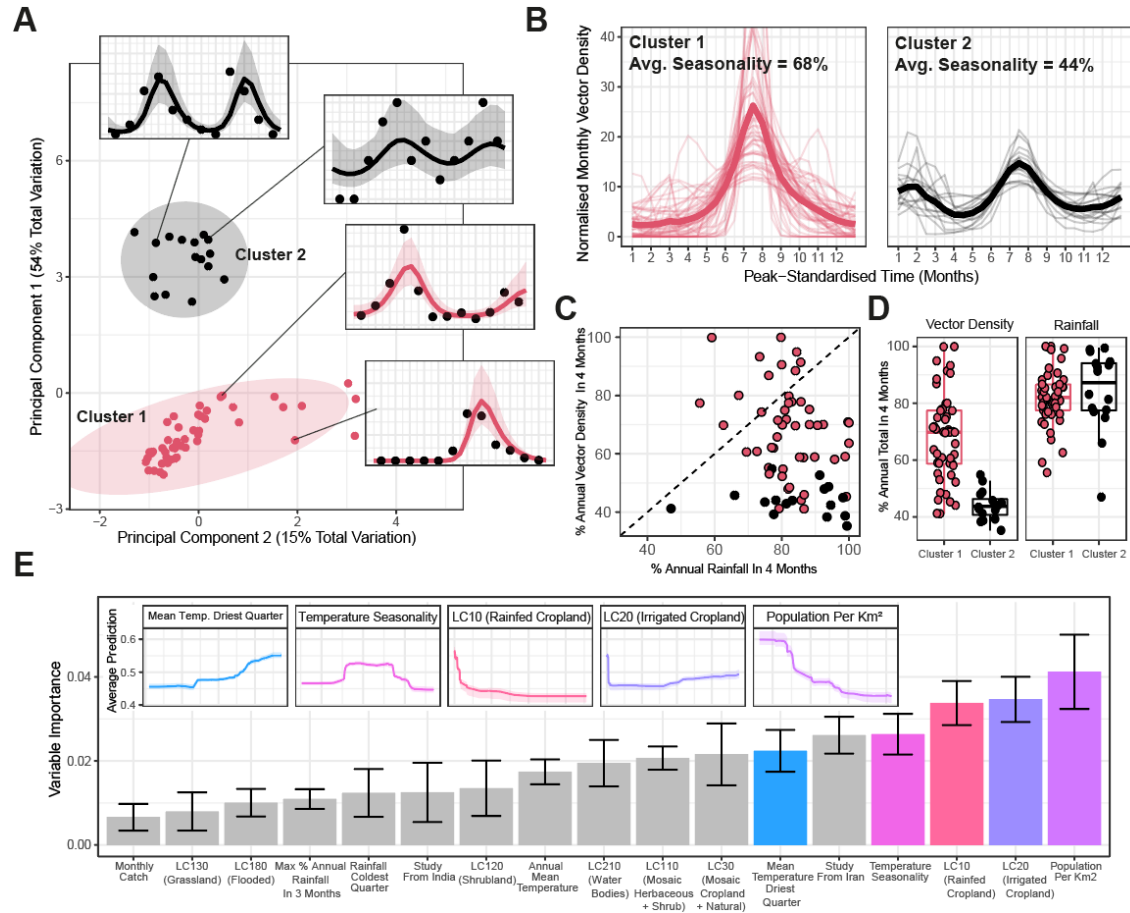
450

451

452

453

Figure 1: Sources and Locations of *Anopheles stephensi* Time-Series Data and Examples for Each Country. (A) Map of the geographical range over which time-series entomological collections have been carried out. Countries with studies are highlighted in light grey, and the locations of individual studies indicated by the individual points, coloured according to country (Afghanistan=red, Djibouti=yellow, India=green, Iran=turquoise, Myanmar=blue and Pakistan=pink). (B) Example *An. stephensi* time-series from each country, with the empirical monthly mosquito catch (black points), fitted gaussian process curves (mean=coloured line, ribbon=95% Bayesian Credible Interval) and monthly rainfall (matching sampling location and year of sampling) for each (light blue bars). The x-axis indicates the month of sampling, the y-axis either the monthly rainfall (left hand side y-axis) or number of vectors caught in each month (right hand side y-axis; note that the absolute number of mosquitoes caught between time-series are not comparable due to variable sampling effort). *n* indicates the number of time-series in each country.



454

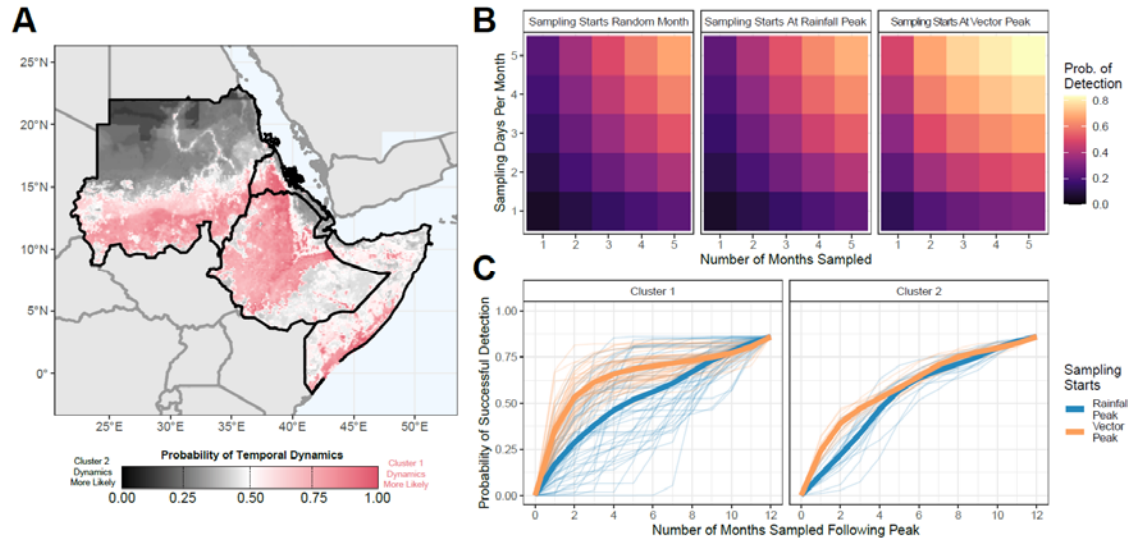
455 **Figure 2: Characterisation and Clustering to Identify Time-Series with Similar**
 456 **Temporal Properties. (A)** Results of principal components analysis (PCA) and k-means
 457 clustering for 2 clusters. Points on main figure indicate individual time-series, with point
 458 colour indicating cluster membership. Ellipsoids demarcate the 75th quantile of the density
 459 associated with each cluster. Principal components 1 and 2 are plotted, together explaining
 460 69% of the total variation in temporal properties across the time-series. **(B)** Time-series
 461 belonging to each cluster. Pale lines represent individual time-series, brighter line the mean
 462 of all the time-series belonging to that cluster – in all cases vector density is normalised to
 463 sum to 1 over the course of the year, and time-standardised so that the highest vector
 464 density for each time-series is arbitrarily set to occur at month 7. **(C)** Plot comparing the
 465 percentage of annual total mosquito catch and percentage of annual total rainfall occurring in
 466 any consecutive 4-month period for each time-series, coloured by cluster membership. **(D)**
 467 Boxplots show the percentage of annual total mosquito catch (left) and annual total rainfall
 468 (right) series occurring any in consecutive 4-month periods for each time-series. Rainfall
 469 data comes from the *CHIRPS* dataset³⁷ and is specific to study location and time-period.
 470 Each point indicates an individual time-series. **(E)** Variable importance plot for each of the
 471 covariates included in the random forest model used to predict cluster membership– bar
 472 height indicates the mean variable importance across the 25 individual iterations of random
 473 forest fitting, with error bars representing the 95% confidence interval. Inset plots are the
 474 partial dependence plots for the top 5 most important variables in the model showing how
 475 the average prediction for Cluster 2 (y-axis, with higher values indicating an increased
 476 probability of Cluster 2 membership) varies with (normalised) variable value (x-axis).

477

478

479

480



481

482 **Figure 3: Possible Seasonal Dynamics of *Anopheles stephensi* Across the Horn of**
483 **Africa, and Consequences for Entomological Surveillance and Monitoring. (A)**

484 Environmental covariates were collated across countries in the Horn of Africa where *An.*
485 *stephensi* has been found, and the random forest classification model from **Fig 2E** used to

486 predict potential temporal dynamics. Map shows the probability of temporal dynamics
487 belonging to Cluster 1 (more seasonal), with pink corresponding to Cluster 1 dynamics being

488 more likely and black indicating Cluster 2 dynamics (more perennial) are more likely,
489 with white indicating both are equally likely. **(B)** For a setting with an annual biting rate of 20,

490 the average probability (across all 65 collated *An. stephensi* temporal profiles) of detecting *An.*
491 *stephensi* (where detection is defined as catching ≥ 1 mosquito) for a range of different

492 sampling efforts (number of consecutive months sampled and number of sampling days in
493 each month) in a setting with an annual biting rate of 20 bites per person. These results were

494 generated for 3 different sampling strategies: i) with sampling starting at a random month in
495 the year (left hand panel, subsequently averaged over all possible sampling start months in

496 the year); ii) with sampling starting in the month of peak rainfall (centre panel); or iii) with
497 sampling starting in the month of peak vector density (right hand panel). **(C)** For setting with

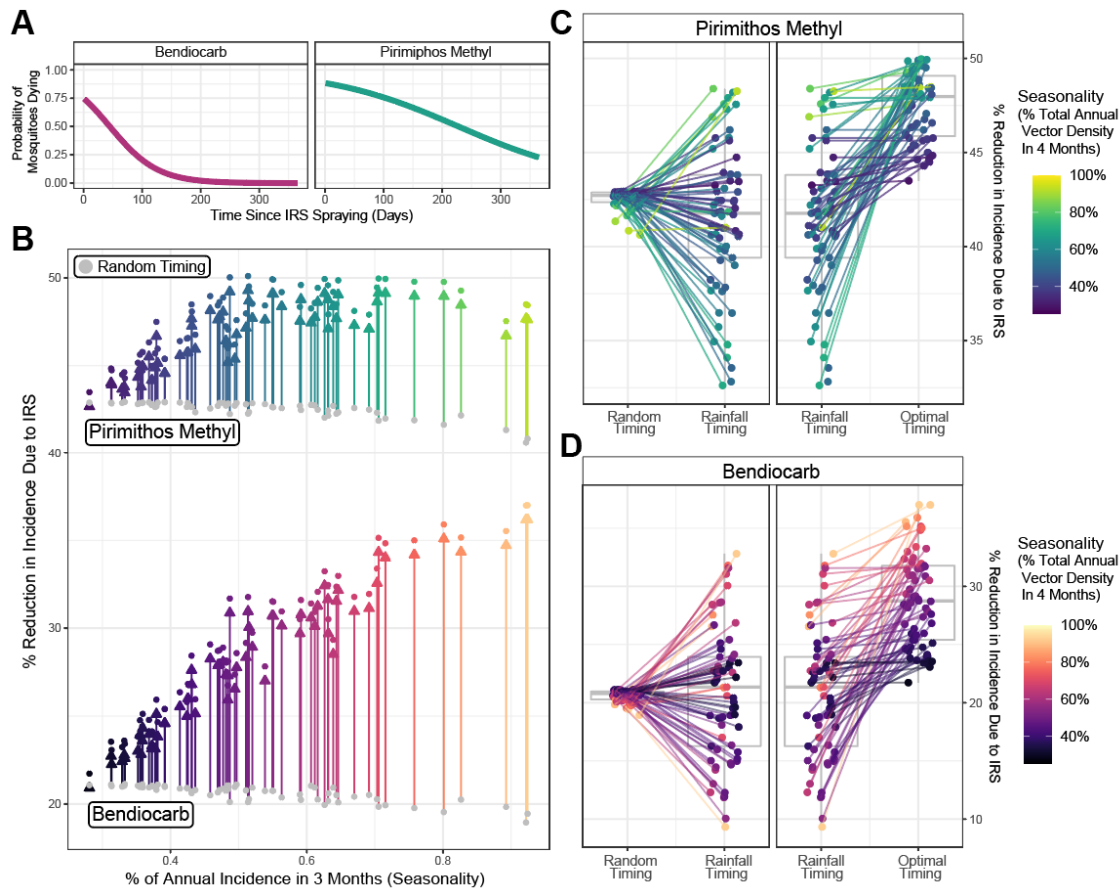
498 an annual biting rate of 20 and a sampling effort of 3 days per month, the cumulative
499 probability of *An. stephensi* detection as a function of the number of consecutive months

500 sampled for each individual time-series, stratified by sampling strategy (starting at peak
501 vector abundance=orange, at peak rainfall=blue) and Cluster. In both panels, pale, thin lines

502 indicate the cumulative probability curve for a specific temporal profile, and thicker lines
503 indicate the average for the specific sampling strategy.

504

505



506

507 **Figure 4: Modelling the Public-Health Impact of Indoor Residual Spraying and the**
 508 **Influence of *Anopheles stephensi* Seasonality. (A)** Probability of mosquitoes dying upon
 509 exposure to each IRS compound in the time-period following spraying⁴² – pink indicates
 510 bendiocarb, turquoise indicates pirimiphos methyl. **(B)** For each temporal profile, the public
 511 health impact of annual IRS campaign with each insecticide according to the timing of the
 512 campaign. Points in grey correspond to the average reduction in incidence occurring from
 513 picking a random month to conduct the IRS campaign for each *An. stephensi* temporal
 514 profile, coloured points indicate the reduction in incidence arising from optimally timing the
 515 IRS campaign relative to the vector density peak for each *An. stephensi* temporal profile
 516 (and coloured arrows indicate the difference). The arrows and coloured points are coloured
 517 according to i) the insecticide used and ii) the degree of *An. stephensi* seasonality in each
 518 temporal profile (defined as the proportion of total annual abundance in any consecutive 4-
 519 month period). **(C)** For pirimiphos methyl and for each *An. stephensi* temporal profile
 520 (coloured points) the percentage reduction in malaria incidence achieved if the IRS
 521 campaign is timed randomly, timed to start when rainfall is at its peak, or optimally timed
 522 based on peak vector density. Points correspond to specific *An. stephensi* temporal profiles
 523 and are coloured according to their degree of seasonality. Boxplot shows the minimum, first
 524 quartile, third quartile and maximum for the different individual projections. **(D)** As for **(C)**,
 525 but for the insecticide bendiocarb.

526 References

- 527 1. Bhatt, S. *et al.* The effect of malaria control on *Plasmodium falciparum* in Africa between 2000 and 2015.
528 *Nature* **526**, 207–211 (2015).
- 529 2. United Nations. Revision of world urbanization prospects. *United Nations: New York, NY, USA* **799**, (2018).
- 530 3. Doumbe-Belisse, P. *et al.* Urban malaria in sub-Saharan Africa: dynamic of the vectorial system and the
531 entomological inoculation rate. *Malar. J.* **20**, 364 (2021).
- 532 4. Robert, V. *et al.* Malaria transmission in urban sub-Saharan Africa. *Am. J. Trop. Med. Hyg.* **68**, 169–176
533 (2003).
- 534 5. Trape, J. F. & Zoulani, A. Malaria and urbanization in central Africa: the example of Brazzaville. Part III:
535 Relationships between urbanization and the intensity of malaria transmission. *Trans. R. Soc. Trop. Med.*
536 *Hyg.* **81 Suppl 2**, 19–25 (1987).
- 537 6. Killeen, G. F., Govella, N. J., Mlacha, Y. P. & Chaki, P. P. Suppression of malaria vector densities and
538 human infection prevalence associated with scale-up of mosquito-proofed housing in Dar es Salaam,
539 Tanzania: re-analysis of an observational series of parasitological and entomological surveys. *Lancet*
540 *Planet Health* **3**, e132–e143 (2019).
- 541 7. De Silva, P. M. & Marshall, J. M. Factors contributing to urban malaria transmission in sub-saharan Africa: a
542 systematic review. *J. Trop. Med.* **2012**, 819563 (2012).
- 543 8. Awolola, T. S., Oduola, A. O., Obansa, J. B., Chukwurar, N. J. & Unyimadu, J. P. *Anopheles gambiae* s.s.
544 breeding in polluted water bodies in urban Lagos, southwestern Nigeria. *J. Vector Borne Dis.* **44**, 241–244
545 (2007).
- 546 9. Kasili, S. *et al.* Entomological assessment of the potential for malaria transmission in Kibera slum of Nairobi,
547 Kenya. *J. Vector Borne Dis.* **46**, 273–279 (2009).
- 548 10. Weiss, D. J. *et al.* Global maps of travel time to healthcare facilities. *Nat. Med.* **26**, 1835–1838 (2020).
- 549 11. Romeo-Aznar, V., Paul, R., Telle, O. & Pascual, M. Mosquito-borne transmission in urban landscapes: the
550 missing link between vector abundance and human density. *Proc. Biol. Sci.* **285**, (2018).
- 551 12. Mourou, J.-R. *et al.* Malaria transmission in Libreville: results of a one year survey. *Malar. J.* **11**, 40 (2012).
- 552 13. Wang, S.-J. *et al.* Rapid Urban Malaria Appraisal (RUMA) IV: epidemiology of urban malaria in Cotonou
553 (Benin). *Malar. J.* **5**, 45 (2006).
- 554 14. Klinkenberg, E., McCall, P., Wilson, M. D., Amerasinghe, F. P. & Donnelly, M. J. Impact of urban agriculture
555 on malaria vectors in Accra, Ghana. *Malar. J.* **7**, 151 (2008).
- 556 15. World Health Organization. Global technical strategy for malaria 2016-2030. 2021 update. *World Health*
557 *Organization: Geneva* (2021).
- 558 16. Sinka, M. E. *et al.* A new malaria vector in Africa: Predicting the expansion range of *Anopheles stephensi*
559 and identifying the urban populations at risk. *Proc. Natl. Acad. Sci. U. S. A.* **117**, 24900–24908 (2020).
- 560 17. Subbarao, S. K., Vasantha, K., Adak, T., Sharma, V. P. & Curtis, C. F. Egg-float ridge number in *Anopheles*
561 *stephensi*: ecological variation and genetic analysis. *Med. Vet. Entomol.* **1**, 265–271 (1987).
- 562 18. Tadesse, F. G. *et al.* *Anopheles stephensi* Mosquitoes as Vectors of *Plasmodium vivax* and *falciparum*,
563 Horn of Africa, 2019. *Emerg. Infect. Dis.* **27**, 603–607 (2021).
- 564 19. Korgaonkar, N. S., Kumar, A., Yadav, R. S., Kabadi, D. & Dash, A. P. Mosquito biting activity on humans &
565 detection of *Plasmodium falciparum* infection in *Anopheles stephensi* in Goa, India. *Indian J. Med. Res.*
566 **135**, 120–126 (2012).
- 567 20. Kumar, A. *et al.* *Anopheles subpictus* carry human malaria parasites in an urban area of Western India and
568 may facilitate perennial malaria transmission. *Malar. J.* **15**, 124 (2016).
- 569 21. Batra, C. P., Adak, T., Sharma, V. P. & Mittal, P. K. Impact of urbanization on bionomics of *An. culicifacies*
570 and *An. stephensi* in Delhi. *Indian J. Malariol.* **38**, 61–75 (2001).
- 571 22. Thomas, S. *et al.* Overhead tank is the potential breeding habitat of *Anopheles stephensi* in an urban
572 transmission setting of Chennai, India. *Malar. J.* **15**, 274 (2016).
- 573 23. Kumar, A. & Thavaselvam, D. Breeding habitats and their contribution to *Anopheles stephensi* in Panaji.
574 *Indian J. Malariol.* **29**, 35–40 (1992).
- 575 24. Faulde, M. K., Rueda, L. M. & Khairah, B. A. First record of the Asian malaria vector *Anopheles stephensi*
576 and its possible role in the resurgence of malaria in Djibouti, Horn of Africa. *Acta Trop.* **139**, 39–43 (2014).
- 577 25. Balkew, M. *et al.* Geographical distribution of *Anopheles stephensi* in eastern Ethiopia. *Parasit. Vectors* **13**,
578 35 (2020).
- 579 26. Ahmed, A. *et al.* Invasive malaria vector *Anopheles stephensi* mosquitoes in Sudan, 2016-2018. *Emerg.*
580 *Infect. Dis.* **27**, 2952–2954 (2021).
- 581 27. Ahmed, A., Khogali, R., Elnour, M.-A. B., Nakao, R. & Salim, B. Emergence of the invasive malaria vector
582 *Anopheles stephensi* in Khartoum State, Central Sudan. *Parasit. Vectors* **14**, 511 (2021).
- 583 28. Ahmed, A., Abubakr, M., Ali, Y., Siddig, E. E. & Mohamed, N. S. Vector control strategy for *Anopheles*
584 *stephensi* in Africa. *Lancet Microbe* **3**, e403 (2022).
- 585 29. Ali, S., Samake, J. N., Spear, J. & Carter, T. E. Morphological identification and genetic characterization of
586 *Anopheles stephensi* in Somaliland. *Parasit. Vectors* **15**, 247 (2022).
- 587 30. Hamlet, A. *et al.* The potential impact of *Anopheles stephensi* establishment on the transmission of
588 *Plasmodium falciparum* in Ethiopia and prospective control measures. *BMC Med.* **20**, 135 (2022).
- 589 31. Feachem, R. G. A. *et al.* Malaria eradication within a generation: ambitious, achievable, and necessary.
590 *Lancet* **394**, 1056–1112 (2019).

- 591 32. ACCESS-SMC Partnership. Effectiveness of seasonal malaria chemoprevention at scale in west and
592 central Africa: an observational study. *Lancet* **396**, 1829–1840 (2020).
- 593 33. Tukei, B. B., Beke, A. & Lamadrid-Figueroa, H. Assessing the effect of indoor residual spraying (IRS) on
594 malaria morbidity in Northern Uganda: a before and after study. *Malar. J.* **16**, 4 (2017).
- 595 34. Tusting, L. S. *et al.* Mosquito larval source management for controlling malaria. *Cochrane Database Syst.*
596 *Rev.* CD008923 (2013).
- 597 35. Whittaker, C. *et al.* The ecological structure of mosquito population seasonal dynamics. *bioRxiv* (2021)
598 doi:10.1101/2021.01.09.21249456.
- 599 36. Carpenter, B. *et al.* Stan: A probabilistic programming language. *J. Stat. Softw.* **76**, 1–32 (2017).
- 600 37. Wright, M. N. & Ziegler, A. ranger: A Fast Implementation of Random Forests for High Dimensional Data in
601 C++ and R. *arXiv [stat.ML]* (2015).
- 602 38. Chawla, N. V., Bowyer, K. W., Hall, L. O. & Kegelmeyer, W. P. SMOTE: Synthetic Minority Over-sampling
603 Technique. *J. Artif. Intell. Res.* **16**, 321–357 (2002).
- 604 39. Griffin, J. T., Ferguson, N. M. & Ghani, A. C. Estimates of the changing age-burden of Plasmodium
605 falciparum malaria disease in sub-Saharan Africa. *Nat. Commun.* **5**, 3136 (2014).
- 606 40. Challenger, J. D. *et al.* Predicting the public health impact of a malaria transmission-blocking vaccine. *Nat.*
607 *Commun.* **12**, 1494 (2021).
- 608 41. Griffin, J. T. *et al.* Reducing Plasmodium falciparum malaria transmission in Africa: a model-based
609 evaluation of intervention strategies. *PLoS Med.* **7**, e1000324 (2010).
- 610 42. Sherrard-Smith, E. *et al.* Systematic review of indoor residual spray efficacy and effectiveness against
611 Plasmodium falciparum in Africa. *Nat. Commun.* **9**, 4982 (2018).
- 612 43. Sumodan, P. K., Kumar, A. & Yadav, R. S. Resting behavior and malaria vector incrimination of Anopheles
613 stephensi in Goa, India. *J. Am. Mosq. Control Assoc.* **20**, 317–318 (2004).
- 614 44. Appawu, M. *et al.* Malaria transmission dynamics at a site in northern Ghana proposed for testing malaria
615 vaccines. *Trop. Med. Int. Health* **9**, 164–170 (2004).
- 616 45. Okello, P. E. *et al.* Variation in malaria transmission intensity in seven sites throughout Uganda. *Am. J.*
617 *Trop. Med. Hyg.* **75**, 219–225 (2006).
- 618 46. Beck-Johnson, L. M. *et al.* The importance of temperature fluctuations in understanding mosquito
619 population dynamics and malaria risk. *R Soc Open Sci* **4**, 160969 (2017).
- 620 47. Mordecai, E. A. *et al.* Thermal biology of mosquito-borne disease. *Ecol. Lett.* **22**, 1690–1708 (2019).
- 621 48. Nagpal, B. N., Srivastava, A., Kalra, N. L. & Subbarao, S. K. Spiracular indices in Anopheles stephensi: a
622 taxonomic tool to identify ecological variants. *J. Med. Entomol.* **40**, 747–749 (2003).
- 623 49. Chavshin, A. R. *et al.* Molecular characterization, biological forms and sporozoite rate of Anopheles
624 stephensi in southern Iran. *Asian Pac. J. Trop. Biomed.* **4**, 47–51 (2014).
- 625 50. Safi, N. H. Z. *et al.* Status of insecticide resistance and its biochemical and molecular mechanisms in
626 Anopheles stephensi (Diptera: Culicidae) from Afghanistan. *Malar. J.* **18**, 249 (2019).
- 627 51. Vatandoost, H. & Hanafi-Bojd, A. A. Indication of pyrethroid resistance in the main malaria vector,
628 Anopheles stephensi from Iran. *Asian Pac. J. Trop. Med.* **5**, 722–726 (2012).
- 629 52. Tiwari, S., Ghosh, S. K., Ojha, V. P., Dash, A. P. & Raghavendra, K. Reduced susceptibility to selected
630 synthetic pyrethroids in urban malaria vector Anopheles stephensi: a case study in Mangalore city, South
631 India. *Malar. J.* **9**, 179 (2010).
- 632 53. Yared, S. *et al.* Insecticide resistance in Anopheles stephensi in Somali Region, eastern Ethiopia. *Malar. J.*
633 **19**, 180 (2020).
- 634 54. Balkew, M. *et al.* An update on the distribution, bionomics, and insecticide susceptibility of Anopheles
635 stephensi in Ethiopia, 2018-2020. *Malar. J.* **20**, 263 (2021).
- 636 55. Massey, N. C. *et al.* A global bionomic database for the dominant vectors of human malaria. *Sci. Data* **3**,
637 160014 (2016).